



Nonfollicular reactivation of bone marrow resident memory CD4 T cells in immune clusters of the bone marrow

Francesco Siracusa^{a,1}, Mairi A. McGrath^{a,1}, Patrick Maschmeyer^a, Markus Bardua^a, Katrin Lehmann^a, Gitta Heinz^a, Pawel Durek^a, Frederik F. Heinrich^a, Mir-Farzin Mashreghi^a, Hyun-Dong Chang^a, Koji Tokoyoda^b, and Andreas Radbruch^{a,2}

^aCell Biology, Deutsches Rheuma-Forschungszentrum (DRFZ) Berlin, 10117 Berlin, Germany; and ^bOsteoimmunology, DRFZ Berlin, 10117 Berlin, Germany

Edited by Kenneth M. Murphy, Washington University, St. Louis, MO, and approved December 26, 2017 (received for review September 4, 2017)

The bone marrow maintains memory CD4 T cells, which provide memory to systemic antigens. Here we demonstrate that memory CD4 T cells are reactivated by antigen in the bone marrow. In a secondary immune response, antigen-specific T cells of the bone marrow mobilize and aggregate in immune clusters together with MHC class II-expressing cells, mostly B lymphocytes. They proliferate vigorously and express effector cytokines, but they do not develop into follicular T-helper cells. Neither do the B lymphocytes develop into germinal center B cells in the bone marrow. Within 10 days, the immune clusters disappear again. Within 30 days, the expanded antigen-specific memory CD4 T cells return to memory niches and are maintained again individually as resting cells. Thus, in secondary immune responses in the bone marrow T-cell memory is amplified, while in germinal center reactions of secondary lymphoid organs humoral memory is adapted by affinity maturation.

bone marrow | tissue-resident CD4 memory T cells | reactivation | immune clusters | secondary immune reaction

It is increasingly recognized that immunological memory is compartmentalized to different areas of the body, with prominent populations of resident memory T cells being located in the bone marrow (1–5) and epithelial tissues such as the skin (6–8), the lung (9–11), and gastrointestinal (12, 13) and reproductive tracts (14, 15). In the bone marrow (BM), CD4 memory T cells specific for systemic antigens are maintained, even when they are absent from spleen and lymph nodes in mice (1), or the blood in humans (4), arguing that these cells are bona fide residents of the BM. BM resident CD4 memory T cells have been shown to provide efficient cognate help for antibody class switching and affinity maturation of antibodies to B lymphocytes in secondary lymphoid organs upon adoptive transfer (1). In the memory phase of an immune response, such memory T cells rest in the BM in terms of proliferation and activation (1, 4) and are maintained individually in “memory niches” organized by mesenchymal stromal cells (5). Here we analyze the reaction of BM resident CD4 memory T cells to antigen. We show that upon rechallenge antigen-specific CD4 memory T cells proliferate within the BM, independently of immigrating cells, and express effector cytokines. The activated T cells migrate to and gather in immune clusters, clustering with MHC class II-expressing cells, mostly mature B lymphocytes. The activated T cells, however, do not show a follicular helper cell phenotype, nor do the B cells express a germinal center phenotype. Within 30 d after reactivation the immune clusters disappear and the amplified antigen-specific CD4 memory T cells rest again in terms of proliferation, individually dispersed throughout the BM. We show here that immunological CD4 memory is amplified within the BM in a nonfollicular fashion in secondary immune reactions.

Results

CD4 Memory T Cells Expand in the BM Following Antigen Reactivation. C57BL/6 mice were immunized with 100 µg lymphocytic choriomeningitis virus (LCMV) GP_{61–80} peptide conjugated with nitrophenol to mouse serum albumin (LCMV-NP-MSA) and with 100 µg poly(I:C) twice, on day 0 and day 14 (without NP-MSA) (Fig. 1A). Antigen-specific CD4 T cells were detected either by MHC class II tetramer staining (LCMV.GP_{66–77}) or according to expression of CD40L and the cytokine IFN-γ upon stimulation with the peptide in vitro. Both methods gave comparable results (Fig. S1A and B). Sixty days after the second immunization, ~40,000 antigen-specific CD4 memory T cells were detected in the BM (Fig. 1C). More than 97% of these cells were resting in the G₀ phase of the cell cycle, since they did not express Ki-67 (Fig. 1B). On day 60 after the second immunization mice were reactivated (boosted) or not with 100 µg LCMV-NP-MSA + 100 µg poly(I:C) and 3 d later the number of antigen-specific T cells in the BM was determined (Fig. 1A). At this time point all of the antigen-specific CD4 T cells in the BM expressed Ki-67, indicating that they were in the G₁ to M phases of the cell cycle (Fig. 1B). Their numbers increased from a mean of 36,182 (± SEM 9,924) to a mean of 959,230 (± SEM

Significance

The bone marrow (BM) harbors critical components of the adaptive immune system able to provide long-lasting protection against pathogens. Among those, CD4 memory T cells are potent helpers of immune reactions in secondary lymphoid organs. Here we analyze their reactivation in the BM in secondary immune reactions. The CD4 memory T cells form clusters with antigen-presenting cells and proliferate vigorously. Although these clusters contain many B lymphocytes, their formation is not dependent on them and no germinal centers develop. Rather, antigen-specific CD4 memory T cells are significantly amplified and, after termination of the immune reaction, they remain in the BM as resting cells. The BM thus provides a dynamic reservoir of CD4 memory T cells, adapting quantitatively to antigenic challenges.

Author contributions: F.S., M.A.M., and A.R. designed research; F.S., M.A.M., P.M., M.B., and K.L. performed research; G.H., P.D., F.F.H., M.-F.M., H.-D.C., and K.T. contributed new reagents/analytic tools; F.S. and M.A.M. analyzed data; and F.S. and M.A.M. wrote the paper.

The authors declare no conflict of interest.

This article is a PNAS Direct Submission.

This open access article is distributed under Creative Commons Attribution-NonCommercial-NoDerivatives License 4.0 (CC BY-NC-ND).

Data deposition: The RNA-sequencing data reported in this paper have been deposited in the Gene Expression Omnibus (GEO) database, <https://www.ncbi.nlm.nih.gov/geo> (accession no. GSE107413).

¹F.S. and M.A.M. contributed equally to this work.

²To whom correspondence should be addressed. Email: radbruch@drfz.de.

This article contains supporting information online at www.pnas.org/lookup/suppl/doi:10.1073/pnas.1715618115/-DCSupplemental.

118,030) within 3 d (Fig. 1C). Boosting the mice with 100 μ g LCMV-NP-MSA only (i.e., without any adjuvant) resulted in a significant amplification of antigen-specific CD4 T cells as well, showing that the expansion of CD4 memory T lymphocytes is independent of the adjuvant (Fig. S1C). In comparison, CD4 memory T cells of the BM that were not specific for LCMV.GP₆₆₋₇₇ did not expand significantly (Fig. 1D and Fig. S1D). A significant expansion was also observed for CD4 memory T cells specific for ovalbumin when reactivated by antigen (Fig. 1E and Fig. S1E). These cells were reactivated 90 d after the second immunization and analyzed 3 d later. Reactivation resulted in a mean of 800,000 (\pm SEM 245,448) of antigen-specific CD4 T cells, compared with 120,000 (\pm SEM 8,092), without reactivation (Fig. 1E). Reactivation also mobilized antigen-specific T cells of the BM. On day 3 after boost the antigen-specific CD4 T cells had significantly up-regulated expression of filamentous actin (F-actin) (Fig. 1F) and were larger in size and polarized in shape (Fig. 1G), compared with resting memory T cells (Fig. 1H). Upon *in vitro* restimulation all of them expressed IFN- γ , with an increased geometric mean fluorescence intensity (GMFI) of 1,021 vs. 473, and about 20% also expressed TNF- α , in the examples given in Fig. S1F and G.

Reactivation of Memory CD4 T Cells in the BM Is Independent of Immigrating Cells. In C57BL/6 mice which had been twice immunized with LCMV GP₆₁₋₈₀ and rested for 60 d the antigen-specific CD4 memory T cells of the BM were heterogeneous with respect to expression of sphingosine-1-phosphate-receptor 1 (S1PR1), a chemokine receptor mediating egress into the blood (16), in that 32% of cells did not express it but rather expressed its antagonist CD69 (Fig. 2A–C) (17). We used the S1PR agonist FTY720 to block egress from and ingress into the BM of T cells, but also of antigen-presenting cells (APCs). Mice were treated with FTY720 (1 mg/kg, *i.p.*) 1 d before boost and for the following 3 d after boost (Fig. S2A). This treatment reduced the number of CD4 T cells in the blood by more than 90% (Fig. 2D) and MHC class II-expressing cells by more than 80% (Fig. S2B), while it did not affect the total cellularity of BM (Fig. S2C). In FTY720-treated mice, reactivated antigen-specific CD4 memory T cells expanded from 67,593 (\pm SEM 14,818) to 634,352 cells (\pm SEM 101,942), that is, ninefold (Fig. 2E). In control (saline-treated) mice, the reactivated cells expanded from 36,182 (\pm SEM 9,924) to 959,230 (\pm SEM 118,030), that is, 26-fold. This difference in expansion rates did not reach statistical significance, indicating that most of the expansion of CD4 T cells was autonomous to BM, with some, statistically not significant, contribution of immigrating T cells. The data also do not indicate an accumulation of antigen-specific CD4 memory T cells in the BM of FTY720-treated mice at day 63, without boost (36,182 \pm SEM 9,924 vs. 67,593 \pm SEM 14,818) (Fig. 2E). BM autonomy in response to systemic antigens was further underlined by the efficient induction of Ki-67 expression in the antigen-specific CD4 T cells, in the presence of FTY720 (Fig. 2F).

Nonfollicular Reactivation of BM CD4 Memory T Cells. Three days after boost, antigen-specific CD4 memory T cells of the BM and spleen from three individual mice were isolated and their global transcriptomes were compared. While principal component 2, accounting for 13% of the differences, reflects experimental variation, reactivated T cells from spleen and BM differ fundamentally in principal component 1, accounting for 70% of the differences (Fig. 3A). Notably, expression of signature genes of follicular helper T cells (T_{FH}) cells, such as Bcl6 and Cxcr5, were significantly less expressed in T cells of the BM, compared with those from spleen (Fig. 3B). In line with this, expression levels of genes described to be up- or down-regulated (18) in T_{FH} vs. non-T_{FH} cells were accordingly up- or down-regulated in reactivated antigen-specific CD4 memory T cells of the BM, compared with the spleen (Tables S1 and S2). According to protein expression

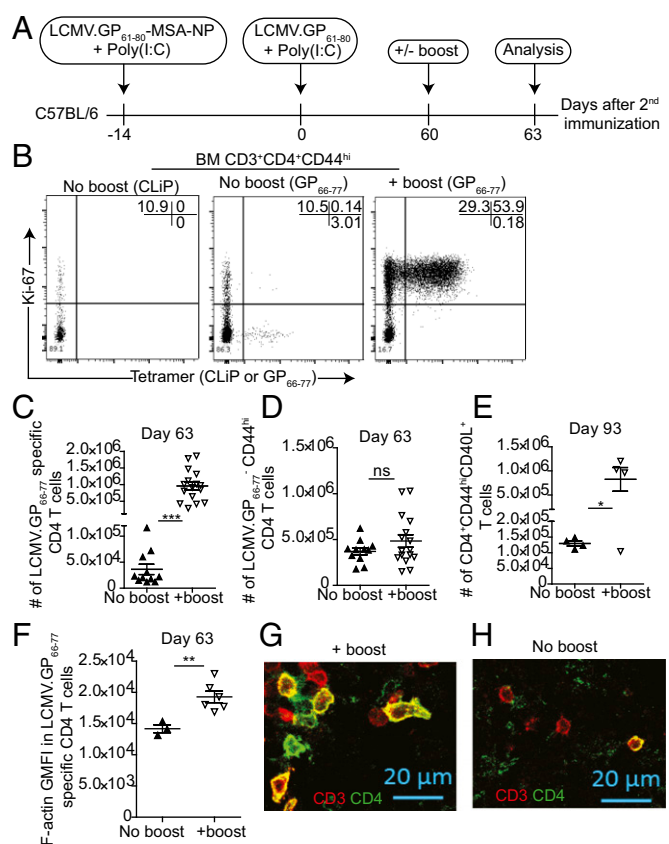


Fig. 1. CD4 memory T cells expand in the BM following antigen reactivation. (A) Schematic showing immunization protocol using LCMV GP₆₁₋₈₀ as antigen. (B) Representative dot plots of Ki-67 vs. LCMV.GP₆₆₋₇₇ loaded tetramer gated on B220⁺Gr1⁺CD3⁺CD4⁺CD44^{hi} viable cells. CLiP loaded tetramer was used as control for staining specificity. (C) Absolute numbers of BM LCMV.GP₆₆₋₇₇-specific CD4 memory T cells on day 63 with (open triangles) and without (filled triangles) boost, as determined by tetramer staining. (D) Absolute numbers of BM CD4 memory-phenotype (LCMV.GP₆₆₋₇₇-negative) T cells on day 63, with (open triangles) and without (closed triangles) boost. (E) Absolute numbers of BM OVA-specific CD4 memory T cells on day 93, with (open triangles) and without (closed triangles) boost, as determined by CD40L up-regulation after *in vitro* restimulation with protein. (F) Expression level of F-actin, stained with phalloidin, in LCMV.GP₆₆₋₇₇-specific CD4 memory T cells on day 63, with (open triangles) and without (closed triangles) boost, as determined by geometric mean based on three to six mice per group. Data shown are from one experiment, representative of two independent experiments. (G) Histology section of activated BM, 3 d after boost, and (H) without boost, showing shape polarization and size of CD4- (green) and CD3- (red) positive T cells. Images were cropped from original images to an equal region size. All images shown are representative of three mice per group. Data in C and D represent the mean of pooled results from three independent experiments \pm SEM, each with three to six mice per group. Data in E are from one experiment with four mice per group. * P < 0.05, ** P < 0.01, *** P < 0.001, as determined by unpaired Student's *t* test. ns, not significant.

of PD-1 and CXCR5, while a defined population of T_{FH} cells could not be detected before the boost (Fig. S2D), about 30% of the reactivated antigen-specific T cells in the spleen qualified as T_{FH} 3 d after the boost. In the BM, a defined population of T_{FH} was not detectable, either before or 3 d after the boost (Fig. 3C and D and Fig. S2D). In line with this, expression of Bcl6 in reactivated T cells of the BM was lower than in reactivated splenic T cells, both at the level of mRNA and protein (Fig. 3B and D). Concurrent with the absence of T_{FH} cells from BM after antigenic challenge we also did not detect B lymphocytes binding high amounts of peanut agglutinin (PNA^{hi}), that is, showing the phenotype of germinal center B cells, 10 d after reactivation,

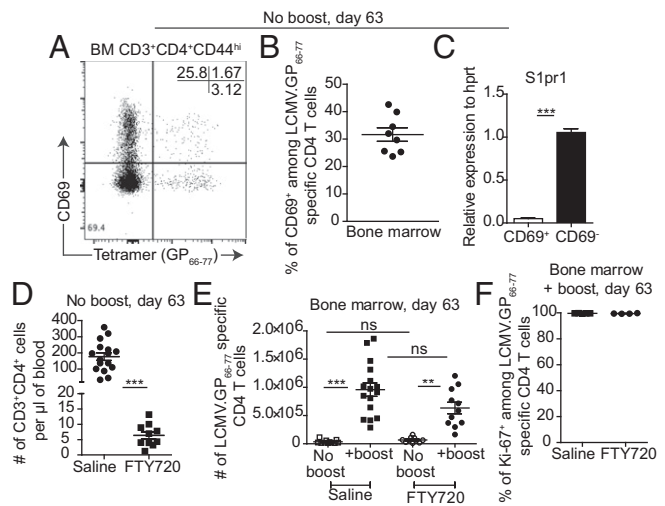


Fig. 2. Reactivation of memory CD4 T cells in the BM is independent of immigrating cells. (A) Representative dot plot of CD69 vs. LCMV.GP₆₆₋₇₇ loaded tetramer gated on B220⁺Gr1⁻CD3⁺CD4⁺CD44^{hi} viable cells on day 63 without boost. (B) Frequency of BM LCMV.GP₆₆₋₇₇-specific CD4 memory T cells expressing CD69 on day 63 without boost. (C) Relative mRNA expression of S1PR1 in FACS-sorted BM CD69⁺ (white bar) or CD69⁻ (black bar) LCMV.GP₆₆₋₇₇-specific CD4 memory T cells on day 63 without boost. (D) Absolute numbers of CD3⁺CD4⁺ T cells per microliter of blood with (squares) and without (circles) FTY720 administration on day 63, without boost. (E) Absolute numbers of BM LCMV.GP₆₆₋₇₇-specific CD4 memory T cells on day 63, with (closed symbols) and without (open symbols) boost and with (circles) and without (squares) FTY720 administration. (F) Proliferative capacity of BM LCMV.GP₆₆₋₇₇-specific CD4 memory T cells as determined by up-regulation of Ki-67 on day 63 after boost, with (circles) and without (squares) FTY720 administration. Data in *B* represent the mean \pm SEM of pooled results from two independent experiments, each with three to five mice per group. Data in *C* are from one experiment with three mice per group. Data in *D* and *E* represent the mean \pm SEM of pooled results from three independent experiments, each with three to five mice per group. Data in *F* are from one experiment, representative of three independent experiments, each with three to five mice per group. ****P* < 0.01, *****P* < 0.001, as determined by one-way ANOVA (*E*) or unpaired Student's *t* test. Saline controls shown in *E* are the same control group as shown in Fig. 1C. ns, not significant.

while they were readily detectable in the spleen at that time (Fig. 3*E* and *F*). Accordingly, PNA^{hi}-binding B lymphocytes were absent before the boost in both the organs (Fig. S2*E*).

Reactivated CD4 Memory T Cells Cluster with B Lymphocytes in Immune Clusters of the BM. Three days after boost, clusters of CD3⁺CD4⁺ T cells and MHC class II-expressing cells appeared in the BM (Fig. 4*A*). Large clusters of T cells and MHC class II-positive cells, with more than 20 CD4 T cells per cluster, were only observed in mice upon antigenic rechallenge. Approximately seven clusters, each one consisting of more than five CD4 T cells, formed in the femoral BM of the reactivated mice, while in the BM of mice which had not been challenged only one out of three femurs showed two clusters (Fig. 4*B*). In the clusters, most CD3⁺CD4⁺ T cells expressed the V α 2 TCR chain, a surrogate marker for LCMV-specific CD4 T cells (Fig. 4*C*), and more than 80% of them contacted MHC class II-expressing cells, while only 30% of the CD3⁺CD4⁺TCRV α 2⁺ T cells outside of the clusters, and individually dispersed through the BM, contacted MHC class II-expressing cells (Fig. 4*D*). In the BM of boosted mice, expression of MHC class II was up-regulated by all MHC class II-expressing cells, around 60% of them B220⁺CD11c⁻ B lymphocytes (Fig. 4*E* and *F*). Among B220⁺MHC-II⁺ cells, 45% were IgM⁺IgD⁺ naive B lymphocytes with a minor component of IgM single-positive (14%) and IgG1- or IgG2a/b-expressing cells

(0.3%) (Fig. S3*A* and *B*), while no clear population of expanding NP-specific B lymphocytes could be detected (Fig. S3*C*). Accordingly, in the clusters around 80% of the MHC class II-expressing cells were B lymphocytes coexpressing IgM and IgD, while no expression of IgG1 or IgG2a/b could be detected

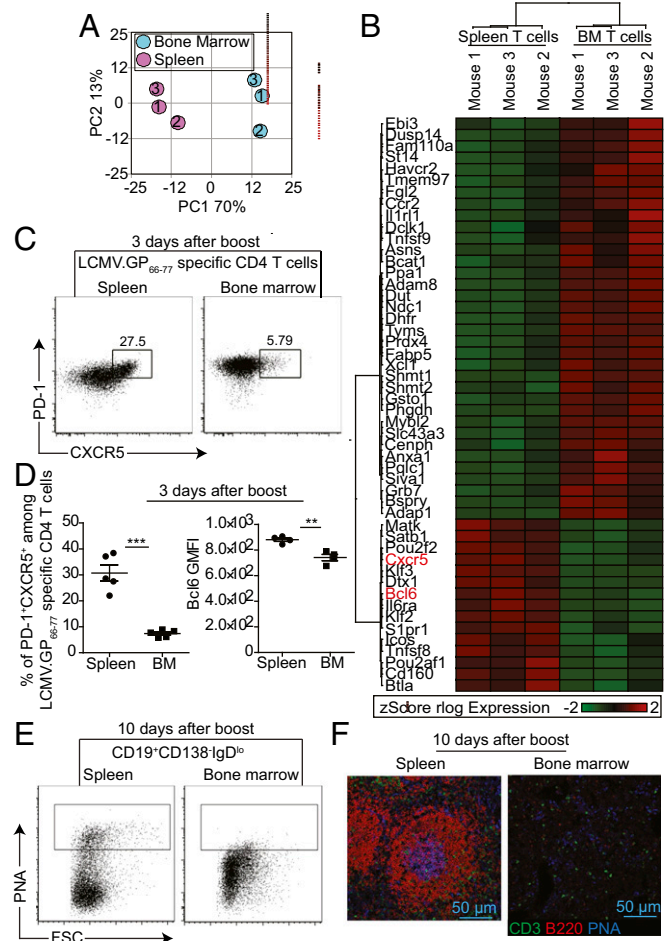


Fig. 3. Nonfollicular reactivation of BM CD4 memory T cells. (A) Principal-component analysis (PCA) of transcriptomes of LCMV.GP₆₆₋₇₇-specific CD4 memory T cells isolated from spleen and BM, 3 d after boost. Each dot represents an individual mouse for a total of three mice per group. (B) Heat map displays differentially expressed genes, which were up- or down-regulated in LCMV.GP₆₆₋₇₇-specific CD4 memory T cells of the BM compared with their splenic counterpart, as determined by RNA sequencing. Shown are Z-score expression levels of selected genes with library-normalized read counts of a minimum of 15 and FC \geq 1.3. Each column represents one individual mouse, for a total of three mice per group. (C) Three days after boost; representative dot plots of PD-1 vs. CXCR5 expression gated on B220⁺Gr1⁻LCMV.GP₆₆₋₇₇⁺CD3⁺CD4⁺CD44^{hi} viable spleen and BM cells. (D) Three days after boost; (Left) frequency of LCMV.GP₆₆₋₇₇-specific CD4 memory T cells coexpressing PD-1 and CXCR5 in spleen (circles) and BM (squares) and (Right) expression level of Bcl6 in LCMV.GP₆₆₋₇₇-specific CD4 memory T cells in spleen (circles) and BM (squares), as determined by geometric mean based on four mice per group. Data shown are from one experiment, representative of two independent experiments. (E) Ten days after boost; representative dot plots of PNA vs. forward scatter (FSC) gated on CD19⁺CD138⁻IgD^{lo} viable cells. (F) Ten days after boost; representative histology sections of spleen and BM with CD3- (green), B220- (red), and PNA- (blue) expressing cells. Images shown are from one mouse, representative of three. Brightness and contrast were similarly adjusted between spleen and BM images. Flow cytometric data in *C* and *E* are from one experiment and representative of three independent experiments, each with four to five mice per group. Data in *D* are shown as mean \pm SEM, ****P* < 0.01, *****P* < 0.001, as determined by unpaired Student's *t* test.

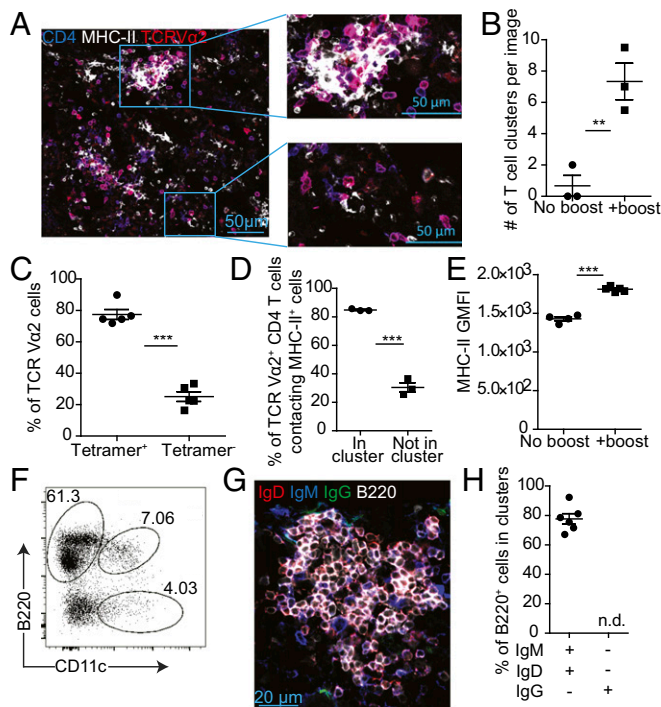


Fig. 4. Reactivated CD4 memory T cells cluster with B lymphocytes in immune clusters of the BM. (A, *Left*) Representative histology section of immune clusters of the BM, 3 d after boost. MHC-II⁺ cells are depicted in white, CD4 cells in blue, and TCR V α 2⁺ cells in red. (*Right*) Zoomed-in area of cluster (*Top*) and noncluster (*Bottom*) of CD4⁺ V α 2⁺ and MHC-II⁺ cells. (B) Number of immune clusters per section of BM calculated for three nonboosted (circles) and three boosted (squares) mice on day 63. (C) Frequency of LCMV.GP₆₆₋₇₇⁺ (tetramer⁺ circles) and LCMV.GP₆₆₋₇₇⁻ (tetramer⁻ squares) CD3⁺CD4⁺CD44^{hi} cells which express TCR V α 2. Data are from one experiment with five mice per group. (D) Frequency of TCRV α 2⁺ CD4⁺ T cells contacting MHC class II-expressing cells inside (circles) or outside (squares) of immune clusters. Approximately 50 V α 2⁺ cells in clusters and 130 V α 2⁺ cells outside of clusters were counted per image for three individual mice and the percentage of cells contacting MHC-II⁺ cells was calculated. (E) Expression level of MHC class II in MHC-II⁺ lymphocytes of the BM with (squares) and without (circles) boost, as determined by geometric mean based on four to five mice per group. Data shown are from one experiment, representative of two independent experiments. (F) Representative dot plot of B220 vs. CD11c gated on MHC-II⁺ viable cells, 3 d after boost. (G) Representative histology section of an immune cluster containing B220⁺IgM⁺IgD⁺ B lymphocytes in the BM, 3 d after boost. B220⁺ cells are shown in white, IgM⁺ cells in blue, IgD⁺ cells in red, and IgG⁺ (IgG1 and IgG2a/b) in green. (H) Frequency of IgD⁺IgM⁺ (circles) and IgD⁻IgM⁺IgG⁺ (IgG1 and IgG2a/b) B220⁺ B cells in immune clusters, 3 d after boost. Two images per mouse for a total of three individual mice were used to calculate the frequencies. Data are shown as mean \pm SEM, ****P* < 0.01, *****P* < 0.001, as determined by unpaired Student's *t* test. n.d., not detected.

(Fig. 4 *G* and *H*). Ten days after boost the immune clusters dissipated and the amplified memory T cells appeared to be dispersed throughout the BM (Fig. *S3E*). Although at this time the consequence of the colocalization of T and B lymphocytes in the immune clusters is not clear, their formation was clearly linked to cognate activation of the antigen-specific CD4 memory T cells, since they were present even when the mice were boosted only with antigen and without any adjuvant (Fig. *S3D*).

B-Cell-Independent Expansion of Antigen-Specific CD4 Memory T Cells in the BM. To investigate whether the B lymphocytes forming the immune clusters in the BM were responsible for the numerical expansion of the antigen-specific CD4 memory T cells, C57BL/6 mice which had been twice immunized with LCMV GP₆₁₋₈₀ and rested for 60 d were i.v. injected 3 d before the boost with a single

dose of 250 μ g anti-CD20 or isotype control, as shown in Fig. *S4A*. Efficient depletion of B lymphocytes was validated the day before the boost. B lymphocytes were reduced by 95% in the blood (Fig. *S4A*). Three days after the boost, numbers of B220⁺MHC-II^{hi} B lymphocytes were also significantly reduced in the BM of anti-CD20-treated mice, compared with the control group (Fig. *S4B* and Fig. *S4B*). In contrast, numbers and frequencies of B220^{lo}MHC-II^{lo} cells expressing CD11c were not affected by the treatment (Fig. *S4B-D*). B-cell depletion did not affect the numerical amplification of antigen-specific CD4 memory T cells in the BM, with 461,229 (\pm 133,631 SEM) vs. 491,178 (\pm 82,031 SEM) reactivated cells in isotype- vs. anti-CD20-treated mice (Fig. *S4C*). The expanding antigen-specific CD4 memory T cells also up-regulated Ki-67 (Fig. *S4E* and *F*). The large immune clusters of T and B lymphocytes, readily detectable in the BM of isotype-control antibody-treated mice (Fig. *S4A*), had disappeared in anti-CD20-treated mice, but smaller clusters of CD3⁺CD4⁺ T and MHC-II⁺ cells were still detected (Fig. *S4B*).

Long-Lasting Amplification of Antigen-Specific CD4 Memory in the BM. On day 90, 30 d after boost, antigen-specific CD4 memory T cells in the BM rested again in terms of proliferation, with 99% of them not expressing Ki-67 (Fig. *S4G*). Their absolute numbers had amplified from 17,540 (\pm SEM 8,657) on day 63 without boost to 2,081,000 (\pm SEM 709,027) on day 90, that is, 118-fold (Fig. *S4G*). Forty percent of the antigen-specific memory T cells were found to express the retention marker CD69 on day 90 (Fig. *S4H*), which was the same frequency as seen on day 63, before boost (Fig. *2A* and *B*). The amplified memory T cells were dispersed individually throughout the BM, and immune clusters were not detectable in femoral BM of the analyzed mice (Fig. *S4D*).

Discussion

Here we have analyzed the reaction of CD4 memory T cells in the BM to antigen. We demonstrate that following antigenic challenge antigen-specific T cells were mobilized and proliferated within the BM. This reaction was autonomous to the BM, since it could not be blocked by the S1PR agonist FTY720. While germinal centers did not form, antigen-specific CD4 memory T cells and IgD⁺IgM⁺ B lymphocytes assembled in de novo formed immune clusters of the BM during the first days after activation. Ten days after reactivation immune clusters had dissolved again; 30 d after reactivation the antigen-specific memory T cells rested again in terms of proliferation, individually dispersed throughout the BM, in significantly amplified numbers. We have previously shown that in the memory

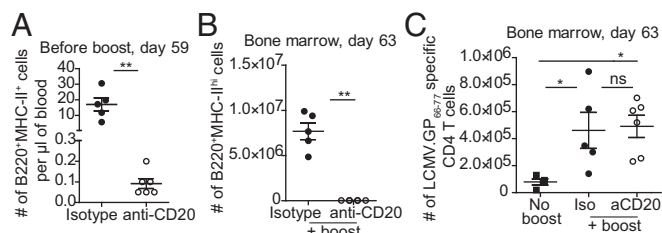


Fig. 5. B cell-independent expansion of antigen-specific CD4 memory T cells in the BM. (A) Absolute numbers of B220⁺MHC-II⁺ cells per microliter of blood with (open circles) and without (closed circles) anti-CD20 administration on day 59, before boost. (B) Absolute numbers of BM B220⁺MHC-II^{hi} cells with (open circles) and without (closed circles) anti-CD20 administration on day 63, with boost. (C) Absolute numbers of BM LCMV.GP₆₆₋₇₇-specific CD4 T cells on day 63 without boost (squares) and with boost with (open circles) or without (closed circles) anti-CD20 administration. Data are shown as mean \pm SEM and are from one experiment with four to six mice per group. **P* < 0.05, ****P* < 0.01, as determined by one-way ANOVA (C) or Mann-Whitney test. ns, not significant.

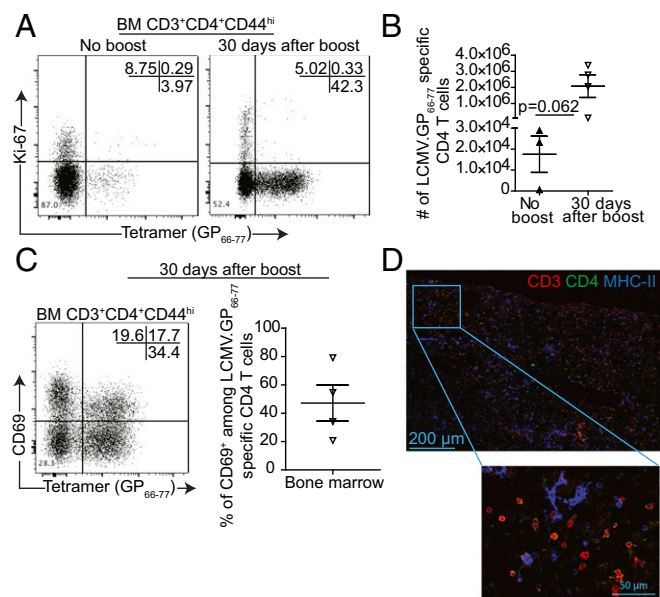


Fig. 6. Long-lasting amplification of antigen-specific CD4 memory in the BM. (A) Representative dot plots of Ki-67 vs. LCMV.GP₆₆₋₇₇ loaded tetramer gated on B220⁻Gr1⁻CD3⁺CD4⁺CD44^{hi} viable cells before boost (day 63) and 30 d after boost (day 90). (B) Absolute number of BM LCMV.GP₆₆₋₇₇-specific CD4 memory T cells before (closed triangles) and 30 d after boost (open triangles). (C) 30 d after boost (day 90); (Left) representative dot plot of CD69 vs. LCMV.GP₆₆₋₇₇ loaded tetramer gated on B220⁻Gr1⁻CD3⁺CD4⁺CD44^{hi} viable cells. (Right) Frequency of BM LCMV.GP₆₆₋₇₇-specific CD4 memory T cells expressing CD69. Data are from one experiment with three to four mice per group. (D) (Top) Tile scan image of BM 30 d after boost (day 90) showing dispersed CD4 (green), MHC-II (blue), and CD3 (red) cells. (Bottom) Zoomed-in image as depicted from box of tile scan image. Images are representative of three mice from one experiment.

phase of an immune response memory T cells reside and rest individually in “memory niches” of the BM, organized by mesenchymal stromal cells which express the cytokine IL-7 (1, 3, 5). At that time, MHC class II-expressing APCs were not found in the vicinity of the CD4 memory T cells, suggesting that antigen does not play a role in their maintenance, in the memory phase of an immune response. Here we show that within 3 d of antigenic rechallenge large aggregates of antigen-specific CD4 T cells and APCs rapidly form in the BM. Most of the APCs are IgD⁺IgM⁺ B lymphocytes. Clusters of T cells and APCs, termed “immune niches” or “immune clusters,” have been described previously in the BM (19–21). However, their frequencies and physiological role remained enigmatic. As we show here, such clusters are rare in, if not absent from, BM of mice, unless their BM CD4 memory T cells are reactivated and mobilized to gather with APCs, mostly B lymphocytes. In the clusters, the CD4 T cells proliferate vigorously, in line with an earlier report (20). We show here that this expansion lasts for several days and results in a numerical amplification of the specific BM memory T cells. Although we did observe an increase in the frequency of Ki-67-expressing tetramer-negative CD4 memory T cells, their numbers did not increase significantly, showing that reactivation of CD4 memory T cells in the BM is cognate, at least with respect to proliferation. In line with this, we observed similar expansion of CD4 memory T cells when mice were boosted with antigen, with and without adjuvant. The role of, and consequences for, the cluster interactions of the B lymphocytes remains elusive; although they do not express IgG, they are not specific for the hapten NP of the reactivating antigen, and they do not develop into germinal center B cells. They are not required for the amplification of CD4 memory T cells, since

ablation of B cells before boost did not impact the expansion of the antigen-specific CD4 memory T cells, although the clusters observed were significantly smaller than they were in the presence of B cells. The present analysis also demonstrates that reactivation of CD4 memory T cells and formation of immune clusters is autonomous to the BM (i.e., independent of immigrating T cells). As the only access to BM is via the blood (22), circulating T cells are restricted to using the S1p-S1pr1 pathway to exit secondary lymphoid organs and enter the blood (17). Blockade of this pathway through the use of the S1PR agonist FTY720 (23–25) did not significantly affect the expansion of LCMV.GP₆₆₋₇₇ tetramer-positive CD4 memory T cells, confirming that these cells had been bona fide residents of the BM and not activated immigrating cells from other organs. Following resolution of the immune response, amplified antigen-specific CD4 memory T cells were no longer proliferating and ~40% of them expressed CD69, a marker of tissue residence (26–28), as had been the case before reactivation. Immune clusters had disappeared by day 10 after challenge, and T cells were dispersed evenly throughout the BM, presumably having returned to their stromal memory niches. The generation of immune clusters containing APCs and BM resident T cells, following antigen reactivation, may be key to the proliferative autonomy seen in the BM. Clusters of T cells with APCs (i.e., immune clusters) are also known to form in other tissues including the female reproductive tract (15), skin (29, 30), gut (31), brain (32), and lung (33–36). Similar to the immune clusters described here for the BM, they are distinct from germinal-center reactions occurring in secondary lymphoid organs (15, 36). Few, if any, of the reactivated CD4 memory T cells of BM exhibited a T_{FH} phenotype, as characterized by expression of CXCR5 and PD-1 and according to their transcriptional signature. Accordingly, PNA^{hi} germinal-center B cells were not detectable in the BM. Although not analyzed here, it is possible that the interaction of B cells and reactivated CD4 memory T cells in the immune clusters of the BM could be expected to result in the generation of “germline memory” (i.e., memory B cells with germline antigen receptors). Indeed, nonhypermutated memory B cells are generated in a T-cell-dependent but not germinal-center- or Bcl6-dependent manner (37–41). This could potentially assign an as-yet-undefined role to the BM in secondary immune responses. In any case, the BM provides a dynamic reservoir of CD4 memory T cells, adapting to repeated antigenic challenge by numerical amplification of specific memory T cells. Overall, here we demonstrate that immunological memory, as conferred by CD4 memory T cells of the BM, is amplified significantly upon antigenic challenge. Cognate reactivated BM resident CD4 memory T cells cluster with B cells in immune clusters of the BM, which are devoid of T_{FH} and germinal-center B cells, highlighting the autonomous nature of the BM for this type of immune reaction.

Experimental Procedures

Mice. All mice were purchased from Charles River and maintained under specific pathogen-free conditions in the mouse facility of the German Rheumatism Research Center Berlin. Experiments were performed according to institutional guidelines and German federal laws on animal protection. Eight-week-old C57BL/6 male mice were immunized i.p. with 100 μg poly(I:C) (Invivogen) and 250 μg OVA (Invivogen) or 100 μg LCMV GP₆₁₋₈₀ (Genecust) coupled to MSA (Merck Millipore) and NP in 200 μL PBS. Two weeks after priming, mice were immunized i.p. again with 100 μg poly(I:C) and 250 μg OVA or 100 μg uncoupled LCMV GP₆₁₋₈₀. Either 60 or 90 d after the last immunization mice were or were not boosted i.p. with 100 μg poly(I:C) and 100 μg OVA or 100 μg LCMV GP₆₁₋₈₀-MSA-NP. Only when indicated, mice were boosted i.p. at day 60 after the last immunization with 100 μg LCMV GP₆₁₋₈₀-MSA-NP alone, without any adjuvant.

FTY720 and Anti-CD20 Treatments. When indicated, mice were treated i.p. with 1 mg/kg FTY720 (Cayman Chemical) or vehicle starting the day before last boost and for the following 3 d until the day of analysis. Normal saline solution was used to dissolve FTY720. When indicated, mice were treated i.v. with a single

injection of 250 μ g anti-CD20 (SA271G2; BioLegend) or isotype control antibody (Rat IgG2b, κ ; BioLegend) 3 d before the last boost. B-cell depletion was checked the day before the boost after bleeding the mice.

Flow Cytometry and Cell Sorting. Flow cytometry and cell sorting were performed as described (42). The following antibodies were used: LCMV.GP₆₆₋₇₇ (DIYKGVYQFKSV) loaded tetramer or hCLiP control (NIH tetramer core facility), anti-CXCR5 (L138D7 or 2G8), anti-CD3 (17A2), anti-CD4 (RM4.4), anti-CD44 (IM7), anti-B220 (RA3.6B2), anti-CD8 (53-6.72), anti-Gr1 (RB6-8C5), anti-CD69 (H1.2F3), anti-PD1 (29F.1A12), anti-MHC class II (M5/114.15.2), anti-CD11c (N418), PNA (Vector Laboratories), anti-TCR $V\alpha 2$ (B20.1), anti-IgM (RMM-1), anti-IgD (11.26c), anti-IgG1 ($\times 56$), anti-IgG2a/b ($\times 57$) or NiP (4-hydroxy-3-iodo-5-nitrophenylacetate), anti-Ki67 (B56), and Phalloidin AF647 (Thermo Fisher Scientific). Viability of cells was assessed via fixable live/dead dye aqua (Thermo Fisher Scientific). Stained samples were acquired on a BD Fortessa (BD Biosciences), MACSQuant (Miltenyi), or Attune NxT (Thermo Fisher Scientific) flow cytometer. For cell sorting, a FACS Aria I (BD Biosciences) cell sorter was used. Flow cytometric data were analyzed using FlowJo software (FlowJo LLC).

Immunofluorescent Staining and Confocal Microscopy. The following primary and secondary reagents were used: anti-CD3 (eBio500A2; eBioscience), anti-CD4 (YTS19.1; DRFZ conjugate), anti-CD44 (IM7; DRFZ conjugate), anti-B220 (RA3.6B2; DRFZ conjugate), anti-MHC II (M5/114; DRFZ conjugate), anti-TCR

$V\alpha 2$ (B20.1; BioLegend), anti-IgM (M41; DRFZ conjugate), anti-IgD (11.26c; DRFZ conjugate), anti-IgG1 ($\times 56$), anti-IgG2a/b ($\times 57$), PNA (Vector Laboratories), and streptavidin-Alexa fluor 488 or 594 (Life Technologies). For nuclear staining, sections were stained with 1 μ g/mL DAPI in PBS. All confocal microscopy was carried out using a Zeiss LSM710 with a 20 \times /0.8 numerical aperture objective lens, image acquisition was performed using Zen 2010 Version 6.0, and images were analyzed by Zen 2012 Light Edition software (Carl Zeiss MicroImaging).

ACKNOWLEDGMENTS. We thank Cassandra Steinkraus, Daniel Schulz, Shintaro Hojo, Tuula Geske, Heidi Hecker-Kia, Heidi Schliemann, and Anette Peddinghaus for their technical help; Andreas Hutloff for scientific discussions; Toralf Kaiser and Jenny Kirsch for cell sorting; and Patrick Thiemann and Manuela Ohde for their assistance with animal care. This work was supported by the Leibniz ScienceCampus Chronic Inflammation (www.chronische-entzuendung.org), European Research Council Advanced Grant IMMOMO [ERC-2010-AdG.20100317 Grant 268987 (to A.R.)], FP7 Marie Curie Initial Training Network Osteoimmune Grant FP7-PEOPLE-2011-ITN-289150 (to F.S.), European Translational Training for Autoimmunity & Immune Manipulation Network (EUTRAIN) Grant FP7-PEOPLE-2011-ITN-289903 (to P.M.), and the state of Berlin and European Regional Development Fund ERDF 2014-2020, EFRE 1.8/11, Deutsches Rheuma-Forschungszentrum (to M.-F.M, P.M., F.F.H, M.B., and M.A.M.).

- Tokoyoda K, et al. (2009) Professional memory CD4⁺ T lymphocytes preferentially reside and rest in the bone marrow. *Immunity* 30:721–730.
- Shinoda K, et al. (2012) Type II membrane protein CD69 regulates the formation of resting T-helper memory. *Proc Natl Acad Sci USA* 109:7409–7414.
- Hanazawa A, et al. (2013) CD49b-dependent establishment of T helper cell memory. *Immunity* 38:524–531.
- Okhrimenko A, et al. (2014) Human memory T cells from the bone marrow are resting and maintain long-lasting systemic memory. *Proc Natl Acad Sci USA* 111:9229–9234.
- Sercan Alp Ö, et al. (2015) Memory CD8⁺ T cells colocalize with IL-7(+)-stromal cells in bone marrow and rest in terms of proliferation and transcription. *Eur J Immunol* 45:975–987.
- Clark RA, et al. (2006) The vast majority of CLA⁺ T cells are resident in normal skin. *J Immunol* 176:4431–4439.
- Jiang X, et al. (2012) Skin infection generates non-migratory memory CD8⁺ T(TRM) cells providing global skin immunity. *Nature* 483:227–231.
- Gebhardt T, et al. (2009) Memory T cells in nonlymphoid tissue that provide enhanced local immunity during infection with herpes simplex virus. *Nat Immunol* 10:524–530.
- Hogan RJ, et al. (2001) Protection from respiratory virus infections can be mediated by antigen-specific CD4⁺ T cells that persist in the lungs. *J Exp Med* 193:981–986.
- Teijaro JR, et al. (2011) Cutting edge: Tissue-retentive lung memory CD4⁺ T cells mediate optimal protection to respiratory virus infection. *J Immunol* 187:5510–5514.
- Wu T, et al. (2014) Lung-resident memory CD8⁺ T cells (TRM) are indispensable for optimal cross-protection against pulmonary virus infection. *J Leukoc Biol* 95:215–224.
- Masopust D, et al. (2010) Dynamic T cell migration program provides resident memory within intestinal epithelium. *J Exp Med* 207:553–564.
- Casey KA, et al. (2012) Antigen-independent differentiation and maintenance of effector-like resident memory T cells in tissues. *J Immunol* 188:4866–4875.
- Shin H, Iwasaki A (2012) A vaccine strategy that protects against genital herpes by establishing local memory T cells. *Nature* 491:463–467.
- Iijima N, Iwasaki A (2014) T cell memory. A local macrophage chemokine network sustains protective tissue-resident memory CD4⁺ T cells. *Science* 346:93–98.
- Matloubian M, et al. (2004) Lymphocyte egress from thymus and peripheral lymphoid organs is dependent on S1P receptor 1. *Nature* 427:355–360.
- Sapozhnikov AJ, Shioh LR, Cyster JG (2010) CD69 suppresses sphingosine 1-phosphate receptor-1 (S1P1) function through interaction with membrane helix 4. *J Biol Chem* 285:22328–22337.
- Liu X, et al. (2012) Bcl6 expression specifies the T follicular helper cell program in vivo. *J Exp Med* 209:1841–1852, S1–S24.
- Feurerer M, et al. (2003) Bone marrow as a priming site for T-cell responses to blood-borne antigen. *Nat Med* 9:1151–1157.
- Feurerer M, et al. (2004) Bone marrow microenvironment facilitating dendritic cell: CD4⁺ T cell interactions and maintenance of CD4⁺ memory. *Int J Oncol* 25:867–876.
- Sapozhnikov A, et al. (2008) Perivascular clusters of dendritic cells provide critical survival signals to B cells in bone marrow niches. *Nat Immunol* 9:388–395.
- Travlos GS (2006) Normal structure, function, and histology of the bone marrow. *Toxicol Pathol* 34:548–565.
- Brinkmann V, et al. (2002) The immune modulator FTY720 targets sphingosine 1-phosphate receptors. *J Biol Chem* 277:21453–21457.
- Mandala S, et al. (2002) Alteration of lymphocyte trafficking by sphingosine-1-phosphate receptor agonists. *Science* 296:346–349.
- Gräler MH, Goetzl EJ (2004) The immunosuppressant FTY720 down-regulates sphingosine 1-phosphate G-protein-coupled receptors. *FASEB J* 18:551–553.
- Shiow LR, et al. (2006) CD69 acts downstream of interferon- α/β to inhibit S1P1 and lymphocyte egress from lymphoid organs. *Nature* 440:540–544.
- Mackay LK, et al. (2015) Cutting edge: CD69 interference with sphingosine-1-phosphate receptor function regulates peripheral T cell retention. *J Immunol* 194:2059–2063.
- Mackay LK, et al. (2013) The developmental pathway for CD103⁺CD8⁺ tissue-resident memory T cells of skin. *Nat Immunol* 14:1294–1301.
- Natsuaki Y, et al. (2014) Perivascular leukocyte clusters are essential for efficient activation of effector T cells in the skin. *Nat Immunol* 15:1064–1069.
- Collins N, et al. (2016) Skin CD4⁺ memory T cells exhibit combined cluster-mediated retention and equilibration with the circulation. *Nat Commun* 7:11514.
- Bergsbaken T, Bevan MJ (2015) Proinflammatory microenvironments within the intestine regulate the differentiation of tissue-resident CD8⁺ T cells responding to infection. *Nat Immunol* 16:406–414.
- Wakim LM, Woodward-Davis A, Bevan MJ (2010) Memory T cells persisting within the brain after local infection show functional adaptations to their tissue of residence. *Proc Natl Acad Sci USA* 107:17872–17879.
- Huh JC, et al. (2003) Bidirectional interactions between antigen-bearing respiratory tract dendritic cells (DCs) and T cells precede the late phase reaction in experimental asthma: DC activation occurs in the airway mucosa but not in the lung parenchyma. *J Exp Med* 198:19–30.
- Veres TZ, et al. (2009) Dendritic cell-nerve clusters are sites of T cell proliferation in allergic airway inflammation. *Am J Pathol* 174:808–817.
- Turner DL, et al. (2014) Lung niches for the generation and maintenance of tissue-resident memory T cells. *Mucosal Immunol* 7:501–510.
- Vu Van D, et al. (2016) Local T/B cooperation in inflamed tissues is supported by T follicular helper-like cells. *Nat Commun* 7:10875.
- Toyama H, et al. (2002) Memory B cells without somatic hypermutation are generated from Bcl6-deficient B cells. *Immunity* 17:329–339.
- Inamine A, et al. (2005) Two waves of memory B-cell generation in the primary immune response. *Int Immunol* 17:581–589.
- Pape KA, Taylor JJ, Maul RW, Gearhart PJ, Jenkins MK (2011) Different B cell populations mediate early and late memory during an endogenous immune response. *Science* 331:1203–1207.
- Kaji T, et al. (2012) Distinct cellular pathways select germline-encoded and somatically mutated antibodies into immunological memory. *J Exp Med* 209:2079–2097.
- Taylor JJ, Pape KA, Jenkins MK (2012) A germinal center-independent pathway generates unswitched memory B cells early in the primary response. *J Exp Med* 209:597–606.
- Cossarizza A, et al. (2017) Guidelines for the use of flow cytometry and cell sorting in immunological studies. *Eur J Immunol* 47:1584–1797.
- Benner R, van Oudenaren A, Koch G (1981) Induction of antibody formation in mouse bone marrow. *Immunological Methods*, eds Lefkowitz I, Pernis B (Academic, New York).
- Kawamoto T (2003) Use of a new adhesive film for the preparation of multi-purpose fresh-frozen sections from hard tissues, whole-animals, insects and plants. *Arch Histol Cytol* 66:123–143.